

BPS Domain Walls in Supersymmetric QCD : Higher Unitary Groups

A.V. Smilga

ITEP, B. Chermushkinskaya 25, Moscow 117218, Russia

and

Service de Physique Théorique de Saclay, 91191 Gif-Sur-Yvette, France

Abstract

We consider the effective lagrangian describing the $\mathcal{N} = 1$ supersymmetric QCD with $SU(N_c)$ gauge group involving $N_f = N_c - 1$ pairs of chiral matter multiplets in fundamental and antifundamental color representations. For this theory in the framework of the effective lagrangian approach, we solve BPS equations for the domain walls interpolating between different vacua. The equations always have a unique solution for the walls interpolating between the chirally asymmetric and a chirally symmetric vacua. For the walls interpolating between different chirally asymmetric vacua, the equations admit two different solutions which exist in a limited range of the mass of the matter fields $m < m_* = \kappa \Lambda_{SQCD}$ where the parameter κ depends on N_c . At $m = m_*$, two branches join together and, at $m > m_*$, no BPS - saturated complex domain walls exist.

1 Introduction

Supersymmetric QCD is the theory involving a gauge vector supermultiplet V and an even number of chiral matter supermultiplets S_i, S'_i ($i = 1, \dots, N_f$ is the flavour index) such that S_i belonging to the fundamental representation of the gauge group $SU(N_c)$ involve left quarks and their scalar superpartners and S'_i belonging to the antifundamental representation involve left antiquarks and their scalar superpartners. The lagrangian of the model reads

$$\mathcal{L} = \left(\frac{1}{4g^2} \text{Tr} \int d^2\theta W^2 + \text{H.c.} \right) + \sum_i \left(\frac{1}{4} \int d^2\theta d^2\bar{\theta} \bar{S}_i e^V S_i + \frac{1}{4} \int d^2\theta d^2\bar{\theta} S'_i e^{-V} \bar{S}'_i \right) - \left(\frac{m_{ij}}{2} \int d^2\theta S'_i S_j + \text{H.c.} \right), \quad (1.1)$$

m_{ij} is the complex mass matrix; color and Lorentz indices are suppressed.

The dynamics of this model attracted the attention of theorists since the beginning of the eighties. In some respects, it is similar to the dynamics of the standard (non-supersymmetric) QCD. If the number of flavours N_f is not too large, it involves confinement, for instance. The model (1.1) has, however, many specific features which are due to supersymmetry. Actually, this theory is in some sense much simpler than the standard QCD — the presence of the extra symmetry allows one to obtain many exact results. The results are especially strong for the extended $\mathcal{N} = 2$ version of the theory [1], but a lot of exact theorems can be derived also for $\mathcal{N} = 1$ theory [2].

The details of the dynamics depend on N_f and on the matter mass matrix m_{ij} . A common feature of all models (1.1) is their nontrivial vacuum structure associated with the spontaneous breaking of a discrete chiral symmetry. Like in the standard QCD, the axial $U_A(1)$ symmetry corresponding to the chiral rotation of the gluino field and present in the tree-level lagrangian (1.1) is broken by anomaly down to Z_{2N_c} . This discrete chiral symmetry can be further broken spontaneously down to Z_2 so that the chiral condensate $\langle \text{Tr} \{ \lambda^\alpha \lambda_\alpha \} \rangle$ (λ_α is a two - component Weyl spinor describing the gluino field) is formed. There are N_c different vacua with different phases of the condensate

$$\langle \text{Tr} \lambda^2 \rangle = \Sigma e^{2\pi i k / N_c}, \quad k = 0, \dots, N_c - 1 \quad (1.2)$$

It was noted recently [3] that on top of N_c chirally asymmetric vacua (1.2), also a chirally symmetric vacuum with zero value of the condensate exists.

The presence of different degenerate physical vacua in the theory implies the existence of domain walls — static field configurations depending only on one spatial coordinate (z) which interpolate between one of the vacua at $z = -\infty$ and another one at $z = \infty$ and minimizing the energy functional. As was shown in [4], in many cases the energy density of these walls can be found exactly due to the fact that the

walls present the BPS-saturated states.¹

One can show (see Refs.[5, 9] for detailed derivation and discussion) that the energy density of a BPS-saturated wall in SQCD satisfies a relation

$$\epsilon = \frac{N_c}{8\pi^2} \left| \langle \text{Tr } \lambda^2 \rangle_\infty - \langle \text{Tr } \lambda^2 \rangle_{-\infty} \right| \quad (1.3)$$

where the subscript $\pm\infty$ marks the values of the gluino condensate at spatial infinities. The RHS of Eq.(1.3) presents an absolute lower bound for the energy of any field configuration interpolating between different vacua.

The relation (1.3) is valid *assuming* that the wall is BPS-saturated. However, whether such a BPS-saturated domain wall exists or not is a non-trivial dynamic question which can be answered only in a specific study of a particular theory in interest.

In Refs.[5, 10, 11] this question was studied in the simplest nontrivial case $N_c = 2$, $N_f = 1$ in the framework of the effective low energy lagrangian due to Taylor, Veneziano, and Yankielowicz [12]. In that case, it is written in terms of the composite colorless chiral superfields

$$\Phi^3 = \frac{3}{32\pi^2} \text{Tr } W^2, \quad X^2 = 2S'S \quad (1.4)$$

and presents a Wess-Zumino model with the superpotential

$$\mathcal{W} = \frac{2}{3} \Phi^3 \left[\ln \frac{\Phi^3 X^2}{\Lambda_{SQCD}^5} - 1 \right] - \frac{m}{2} X^2 \quad (1.5)$$

The results are the following:

1. For any value of the mass of the matter fields m , there are domain walls interpolating between a chirally asymmetric and the chirally symmetric vacua. They are BPS - saturated.
2. There are also complex BPS solutions interpolating between different chirally asymmetric vacua. But they exist only if the mass is small enough $m \leq m_* = 4.67059 \dots \Lambda_{SQCD}$. When $m > m_*$, BPS walls are absent.
3. In a narrow range of masses $m_* < m \leq m_{**} \approx 4.83 \Lambda_{SQCD}$, complex domain walls still exist, but they are not BPS saturated anymore. At $m > m_{**}$, there are no such walls whatsoever.

All these results were obtained by solving numerically the first order BPS equations

$$\partial_z \phi = e^{i\delta} \partial \bar{\mathcal{W}} / \partial \bar{\phi}, \quad \partial_z \chi = e^{i\delta} \partial \bar{\mathcal{W}} / \partial \bar{\chi} \quad (1.6)$$

¹Such BPS-saturated walls were known earlier in 2-dimensional supersymmetric theories (they are just solitons there) [6, 7] and were considered also in 4-dimensional (non-gauge) theories in stringy context [8].

associated with the TVY lagrangian ² (see Refs.[5, 9] for details) and/or the equations of motion for the profile of the wall with the proper boundary conditions. Technically, the easiest problem was to study the point 1 of the list above [5]: the phase of the complex scalar fields ϕ and χ (the lowest components of the superfields Φ and X) does not change along such a wall and can be set to zero which simplifies the equations considerably. Point 2 is a bit more difficult [10]: one has to solve here essentially complex BPS equations to obtain essentially complex solutions. Point 3 is still more difficult: we have to solve the equations of motion which are of the second order [11].

In this paper, we address the same issues for theories with higher unitary gauge groups. In particular, we study the points 1 and 2 and show that the results are basically the same: the real walls are always BPS saturated, and they exist for all masses while the complex BPS equations have non-trivial solutions only in the limited range of mass: $m \leq m_* = .28604 \dots \Lambda_{SQCD}$ for $SU(3)$, $m \leq m_* = .07539 \dots \Lambda_{SQCD}$ for $SU(4)$, etc. When $m > m_*$, the solutions are absent. A study of the corresponding equations of motion which would allow us to find the form and the properties of non-BPS walls is now in progress.

The paper is organized as follows. In the next section we write down the effective lagrangian for the model in interest, discuss its vacuum structure and some generalities concerning the wall solutions. In Sect. 3, we find the BPS solutions for the real walls. Complex walls in the Higgs phase (in the limit $m \rightarrow 0$) are discussed in Sect. 4. In Sect. 5, we analyze the case of small finite masses and find the solution as a series in a small Born–Oppenheimer parameter. Numerical results for the complex walls for general values of mass are presented in Sect. 6. In Sect. 7, we discuss the properties of a peculiar “lower” BPS solution at small masses. Summary and some general discussion is the subject of the last section.

2 The model

In this paper, we restrict ourselves with studying the model (1.1) with $N_f = N_c - 1$. We also choose the simplest form for the mass matrix $m_{ij} = m\delta_{ij}$. When m is small (much smaller than Λ_{SQCD}), the expectation values of the squark fields $\langle s_i \rangle$, $\langle s'_i \rangle$ in chirally asymmetric vacua are large. It turns out that, for different flavours, the vacuum expectation values have different colour orientations. Up to overall flavour and colour rotations, one may choose [2]

$$\begin{aligned} \langle s_1 \rangle &= \frac{v}{\sqrt{2}} \begin{pmatrix} 1 \\ 0 \\ \dots \\ 0 \end{pmatrix}, \dots, \langle s_{N_c-1} \rangle = \frac{v}{\sqrt{2}} \begin{pmatrix} 0 \\ \dots \\ 1 \\ 0 \end{pmatrix} \\ \langle s'_1 \rangle &= \frac{v}{\sqrt{2}}(1, 0, \dots), \dots, \langle s'_{N_c-1} \rangle = \frac{v}{\sqrt{2}}(0, \dots, 1, 0) \end{aligned} \quad (2.1)$$

²In the $SU(2)$ case, we should set $\delta = 0$ or $\delta = \pi$ depending on the “direction” of the wall.

with $v \propto m^{-1/2N_c}$; columns and rows display the colour structure. A set of Higgs averages (2.1) break the $SU(N_c)$ colour symmetry completely: all the gauge bosons acquire a large mass. When m is small, v is large, the effective coupling $g(v)$ is small and the vacuum state has a trivial perturbative nature. One can say that the theory is in a weak-coupling Higgs phase.

The effective TVY lagrangian is written now in terms of the composite colorless fields

$$\Phi^3 = \frac{3}{32\pi^2} \text{Tr } W^2, \quad \mathcal{M}_{ij} = 2S'_i S_j \quad (2.2)$$

It is again a Wess–Zumino model with the superpotential

$$\mathcal{W} = \frac{2}{3} \Phi^3 \left[\ln \frac{\Phi^3 \det \mathcal{M}}{\Lambda_{SQCD}^{2N_c+1}} - 1 \right] - \frac{m}{2} \text{Tr } \mathcal{M} \quad (2.3)$$

The superpotential is rigidly fixed from the requirement that the conformal and the chiral anomaly of the theory (1.1) under consideration are reproduced correctly. For all vacuum states, the matrix $\langle s'_i s_j \rangle$ of the vacuum expectation values is proportional to unity: $\langle s'_i s_j \rangle = C \delta_{ij}$. The same is true for the domain walls interpolating between different vacua. So, we can safely impose the constraint $\mathcal{M}_{ij} = X^2 \delta_{ij}$ and study the Wess–Zumino model with just two superfields Φ and X and the superpotential

$$\mathcal{W} = \frac{2}{3} \Phi^3 \left[\ln \{ \Phi^3 X^{2(N-1)} \} - 1 \right] - \frac{m}{2} (N-1) X^2 \quad (2.4)$$

($N \equiv N_c$ and we have set $\Lambda_{SQCD} \equiv 1$). The corresponding potential for the lowest components ϕ, χ of the superfields Φ, X is

$$U(\phi, \chi) = \left| \frac{\partial \mathcal{W}}{\partial \phi} \right|^2 + \left| \frac{\partial \mathcal{W}}{\partial \chi} \right|^2 = 4 \left| \phi^2 \ln \{ \phi^3 \chi^{2(N-1)} \} \right|^2 + (N-1)^2 \left| m\chi - \frac{4\phi^3}{3\chi} \right|^2 \quad (2.5)$$

The potential (2.5) has $N+1$ degenerate minima. One of them is chirally symmetric $\phi = \chi = 0$ (one should take care, of course, that the ratio ϕ^3/χ would also tend to zero in the limit $\phi \rightarrow 0, \chi \rightarrow 0$). There are also N chirally asymmetric vacua

$$\chi_k = \rho_* e^{i\pi k/N}, \quad \phi_k = R_* e^{-\frac{2i(N-1)\pi k}{3N}} \quad (2.6)$$

with

$$\rho_* \equiv v = \left(\frac{4}{3m} \right)^{1/(2N)}, \quad R_* = \left(\frac{3m}{4} \right)^{(N-1)/(3N)} \quad (2.7)$$

The values of the superpotential (2.4) at the minima are $\mathcal{W}_{\text{sym}} = 0$ and

$$\mathcal{W}_k = -\frac{N}{2} \left(\frac{4m^{N-1}}{3} \right)^{1/N} e^{2\pi i k/N} \quad (2.8)$$

There are also the minima with the inverse sign of χ (and the appropriately chosen phase of ϕ), but they are physically the same as the minima (2.6): the vacuum expectation values of the gauge invariant operators $\langle \text{Tr } \lambda^2 \rangle = (32\pi^2/3) \langle \phi^3 \rangle$ and $\langle 2s'_i s_j \rangle = \langle \chi^2 \rangle \delta_{ij}$ are the same. The vacuum values of the gluino condensate are $\langle \text{Tr } \lambda^2 \rangle_{\text{sym}} = 0$ and

$$\langle \text{Tr } \lambda^2 \rangle_k = 8\pi^2 \left(\frac{4m^{N-1}}{3} \right)^{1/N} e^{2\pi ik/N} \quad (2.9)$$

To study the domain wall configurations, we should add to the potential (2.5) the kinetic term which we choose in the simplest possible form

$$\mathcal{L}_{\text{kin}} = |\partial\phi|^2 + |\partial\chi|^2 \quad (2.10)$$

(it follows from the term $1/4 \int d^4\theta \bar{\Phi}\Phi + 1/4 \int d^4\theta \bar{X}X$ in the superlagrangian) and solve the equations of motion with appropriate boundary conditions. Following Refs.[5, 10], we will look in this paper only for the solutions of the more simple BPS equations (1.6) which are of the first order.

The model involves two types of walls. Some of them interpolate between the chirally symmetric vacuum and a chirally asymmetric one. There are N such walls which transform into each other under trivial Z_N phase rotation. It is convenient to choose the chirally asymmetric vacuum with $k = 0$ in which case the wall solution is purely *real*.

Other walls interpolate between chirally asymmetric vacua (2.6) with different k . We will restrict ourselves with studying the walls interpolating between *adjacent* asymmetric vacua, say, between the vacuum with $k = 0$ and the vacuum with $k = 1$. For $N = 2, 3$, it is the whole story but, starting from $N = 4$, also the walls connecting the vacua with $k = 0$ and $k = 2$ etc. may appear. All such solutions are essentially *complex*.

The value of δ to be chosen in Eq.(1.6) depends on the wall solution we are going to find. To fix it, note that the equations (1.6) admit an integral of motion:

$$\text{Im}[\mathcal{W}(\phi, \chi)e^{-i\delta}] = \text{const} \quad (2.11)$$

Indeed, we have

$$e^{-i\delta} \partial_z \mathcal{W} = e^{-i\delta} \left(\frac{\partial \mathcal{W}}{\partial \phi} \partial_z \phi + \frac{\partial \mathcal{W}}{\partial \chi} \partial_z \chi \right) = \left| \frac{\partial \mathcal{W}}{\partial \phi} \right|^2 + \left| \frac{\partial \mathcal{W}}{\partial \chi} \right|^2 = e^{i\delta} \partial_z \bar{\mathcal{W}}$$

The real wall connects the vacua with $\mathcal{W} = 0$ and $\mathcal{W} = -N/2(4m^{N-1}/3)^{1/N}$. These boundary conditions are consistent with Eq.(2.11) only if $e^{i\delta} = \pm 1$ (the sign depends on whether the walls goes from the symmetric vacuum to the asymmetric one when z goes from $-\infty$ to $+\infty$ or the other way round).

A complex wall connects the vacua where the superpotential (2.4) acquires non-zero values with different complex phases. For the wall connecting the vacua with $k = 0$ and $k = 1$, the condition (2.11) is consistent with the choice $\delta = \pi/N \pm \pi/2$ depending on the direction of the wall.

Bearing in mind Eqs. (1.3, 2.9), the energy densities of the BPS walls are

$$\epsilon_r = N \left(\frac{4m^{N-1}}{3} \right)^{1/N} \quad (2.12)$$

for the real walls and

$$\epsilon_c = 2N \sin \frac{\pi}{N} \left(\frac{4m^{N-1}}{3} \right)^{1/N} = 2\epsilon_r \sin \frac{\pi}{N} \quad (2.13)$$

for the complex walls.

Before coming to grips with finding the numerical solutions of the BPS equations for an arbitrary value of mass, let us discuss what happens in the limiting cases $m \rightarrow \infty$ and $m \rightarrow 0$ where the situation is considerably simplified.

Consider first the case of large masses. In this case, one can integrate the heavy matter fields out and write the effective lagrangian for the composite chiral superfield Φ . Technically, one should use the Born–Oppenheimer procedure and to freeze down the matter field χ so that the large second term in the potential (2.5) disappear. Proceeding in supersymmetric way, we get $X^2 = 4\Phi^3/3m$. Substituting it in the first term, we obtain the Veneziano–Yankielowicz effective lagrangian [13] which is the Wess–Zumino model for the single chiral superfield Φ with the superpotential

$$\mathcal{W} = \frac{2N}{3} \Phi^3 [\ln \Phi^3 - 1] \quad (2.14)$$

where Φ is measured now in the units of

$$\Lambda_{SYM} = \left(\frac{3m}{4} \right)^{(N-1)/3N} \Lambda_{SQCD}^{(2N+1)/3N}$$

The corresponding potential is

$$U(\phi) = |\partial\mathcal{W}/\partial\phi|^2 = 4N^2 |\phi^4| |\ln \phi^3|^2 \quad (2.15)$$

This expression is not yet well defined: the logarithm has many sheets, and one should specify first what particular sheet should be taken. An accurate analysis taking into account the fact that the topological charge $\nu \propto \int \text{Tr}\{G^2 \tilde{G}^2\} d^4x$ in the original theory (1.1) is quantized to be integer reveals that the true potential is glued out of N such sheets [3, 5].³ The gluing occurs when the phase of the

³ Quite an analogous situation holds in the Schwinger model: the true bosonized lagrangian (in the Schwinger model it is just *equivalent* to the original theory) is glued out of several branches when taking into account the effects due to quantization of topological charge [14].

expression under logarithm reaches the values $\pm\pi/N$ [3, 5]:

$$\begin{aligned}
\ln \phi^3 &\equiv \ln |\phi^3| + i \arg(\phi^3), & \arg(\phi^3) &\in \left(-\frac{\pi}{N}, \frac{\pi}{N}\right) \\
\ln \phi^3 &\equiv \ln |\phi^3| + i \left[\arg(\phi^3) - \frac{2\pi}{N} \right], & \arg(\phi^3) &\in \left(\frac{\pi}{N}, \frac{3\pi}{N}\right) \\
&\dots \\
\ln \phi^3 &\equiv \ln |\phi^3| + i \left[\arg(\phi^3) - \frac{2(N-1)\pi}{N} \right], \\
&\arg(\phi^3) \in \left(\frac{\pi(2N-3)}{N}, \frac{\pi(2N-1)}{N}\right)
\end{aligned} \tag{2.16}$$

(remind that only the field $\phi^3 \propto \text{Tr } \lambda^2$, not ϕ itself has a direct physical meaning). Bearing the prescription (2.16) in mind, the potential (2.15) has $N + 1$ minima as it should: $\phi_{\text{sym}} = 0$ and $\phi_k = e^{2i\pi k/3N}$.

As was shown in Ref.[5], the BPS equations involve only the real solutions with the chirally symmetric vacuum at one of the boundaries in this case. Non-trivial complex domain walls connecting different chirally asymmetric vacua are absent.

Consider now the case of small masses. In this case, chirally asymmetric vacua are characterized by large expectation values of the matter scalar field $\langle \chi \rangle \sim \rho_* \propto m^{-1/2N}$. Again, the theory involves two different energy scales, and one can tentatively integrate out heavy fields and to write down the Wilsonian effective lagrangian describing only light degrees of freedom. Proceeding in the Born–Oppenheimer spirit, we should freeze now the heavy field ϕ in the potential (2.5) so that the large first term in the potential acquire its minimum (zero) value. In contrast to the large mass situation, this can now be achieved in two ways: either by setting $\phi = 0$ or by setting $\phi^3 \chi^{2(N-1)} = 1$. In the first case, we will obtain the effective lagrangian describing the dynamics of the chirally symmetric phase which is just the lagrangian of free light chiral field X involving χ and its superpartner.

The second choice results in the lagrangian describing the dynamics of the chirally asymmetric phases. It is the lagrangian of the Wess–Zumino model with a single chiral superfield X and a non-trivial superpotential

$$\mathcal{W} = -\frac{2}{3X^{2(N-1)}} - \frac{m}{2}(N-1)X^2. \tag{2.17}$$

This lagrangian is well known and was obtained earlier from instanton and/or from holomorphy considerations [2]. The corresponding potential $U = |\partial W/\partial \chi|^2$ has N different non-trivial minima at $\chi_k = \rho_* e^{i\pi k/N}$. When $m \ll 1$, a large expectation value $\langle \chi \rangle$ results in breaking down the gauge symmetry of the original theory by the Higgs mechanism: the theory is in the Higgs phase.

The BPS equations corresponding to the superpotential (2.17) admit non-trivial complex domain wall solutions connecting different asymmetric vacua. When $N = 2$, the solution can be found analytically [5]. For $N \geq 3$, there are only numerical solutions which will be presented and discussed in Sect. 4 of the paper.

In this approach, we are not able, however, to study the real domain walls interpolating between the chirally symmetric and a chirally asymmetric vacua. Such a wall corresponds to going through a high energy barrier separating two kind of vacua. It is a remarkable consequence of supersymmetry and of the related BPS condition (1.3) that the energy of such a wall is still not large. For $N = 2$, such walls were analyzed in Ref.[5]. In the next section, we do the same for arbitrary N and reach the same conclusions.

Thereby, the physical situation in the limits $m \rightarrow 0$ and $m \rightarrow \infty$ is somewhat different. In both cases, we have $N + 1$ different vacua. However, an analog of nontrivial complex walls connecting different asymmetric vacua which are present at small masses, is absent when the mass is large. In the latter case, only real walls are present. It is therefore very interesting to understand what happens in between, at intermediate values of masses, and how the transition from one regime to another occurs. That was the main motivation for our study.

All the calculations were performed in the framework of the effective theory with the potential (2.5). The status of this effective theory is somewhat more uncertain than that of (2.17) — for general value of mass, the TVY effective lagrangian is not Wilsonian; light and heavy degrees of freedom are not nicely separated. But it possesses all the relevant symmetries of the original theory and satisfies the anomalous Ward identities for correlators at zero momenta. We think that the use of the TVY lagrangian is justified as far as the vacuum structure of the theory is concerned.

3 Real Walls

The BPS equations (1.6) with the superpotential (2.4) have the form

$$\begin{aligned}\phi' &= e^{i\delta} \cdot 2\bar{\phi}^2 \ln\{\bar{\phi}^3 \bar{\chi}^{2(N-1)}\} \\ \chi' &= e^{i\delta} \cdot (N-1) \left[\frac{4\bar{\phi}^3}{3\bar{\chi}} - m\bar{\chi} \right]\end{aligned}\tag{3.1}$$

($O' \equiv \partial_z O$). To find the wall interpolating between $\phi = \chi = 0$ at $z = -\infty$ and $\phi = R_*, \chi = \rho_*$ at $z = \infty$, we have to choose $\delta = \pi$ (or $\delta = 0$ for the wall going in the opposite direction). With this choice and the boundary conditions given, the solutions $\phi(z)$ and $\chi(z)$ are going to be real so that we have a simple system of just two first-order differential equations.

For all N , the dynamics of this system is quite similar to that in the case $N = 2$ studied in Ref.[5]. The solution exists for all masses. For large m , the heavy matter field can be integrated out, and we arrive at the BPS equation for the supersymmetric gluodynamics

$$\phi' = -2N\phi^2 \ln(\phi^3/R_*^3)\tag{3.2}$$

The solution of this equation with the boundary conditions $\phi(-\infty) = 0$, $\phi(\infty) = R_*$ can be expressed into integral logarithms.

As was the case for $N = 2$, the solution of the system (3.1) can be found in an analytic form also for small masses. The wall trajectory consists then in two distinct regions. On the first stage, only the light field χ is changed, $\chi(z) = \rho_* e^{mz}$, while the field ϕ stays frozen at zero. Then, at $z = 0$, the trajectory abruptly turns. $\chi(z)$ stays frozen at its vacuum value ρ_* and the equation for $\phi(z)$ is reduced to $\phi' = -2\phi^2 \ln\{\phi^3 \rho_*^{2(N-1)}\}$ which is the same as Eq.(3.2). The second stretch is much thinner than the first one, its width being of order $R_*^{-1} \propto m^{-(N-1)/3N}$. It is on this second stage when the high and narrow potential barrier between the regions $\phi \sim 0$ and $\phi \sim \chi^{-2(N-1)/3}$ is penetrated. The width of the first stretch is $\sim 1/m$ and it carries the fraction $(N-1)/N$ of the total energy (2.12). Correspondingly, the second thin stretch carries the fraction $1/N$ of the total energy.

In the intermediate range of masses, the solution has to be found numerically. Parametric plots in the (ϕ, χ) plane for $N = 3$ and different values of m are drawn in Fig. 1.

4 Domain Walls in Higgs Phase

We have got to solve the BPS equations

$$\chi' = e^{-i\pi(N-2)/2N} \frac{\partial \bar{\mathcal{W}}}{\partial \bar{\chi}}, \quad (4.1)$$

where \mathcal{W} is the superpotential (2.17), with the boundary conditions

$$\chi(-\infty) = \rho_*; \quad \chi(\infty) = \rho_* e^{i\pi/N}; \quad (4.2)$$

It is convenient to introduce polar variables $\chi = \rho e^{i\alpha}$. The equations (4.1) acquire the form

$$\begin{aligned} \rho' &= (N-1) \left\{ m\rho \sin \gamma - \frac{4}{3\rho^{2N-1}} \sin[\gamma(N-1)] \right\} \\ \gamma' &= 2(N-1) \left\{ m \cos \gamma + \frac{4}{3\rho^{2N}} \cos[\gamma(N-1)] \right\} \end{aligned} \quad (4.3)$$

where $\gamma \equiv 2\alpha - \pi/N$ changes from $\gamma = -\pi/N$ at $z = -\infty$ to $\gamma = \pi/N$ at $z = \infty$. For $N = 2$, these equations were solved in Ref.[5]. The solution is analytic:

$$\begin{aligned} \rho(z) &= \rho_* \\ \tan \gamma(z) &= \sinh[4m(z - z_0)] \end{aligned} \quad (4.4)$$

or in the complex form:

$$\chi(z) = \rho_* \frac{1 + ie^{4m(z-z_0)}}{\sqrt{1 + e^{8m(z-z_0)}}} \quad (4.5)$$

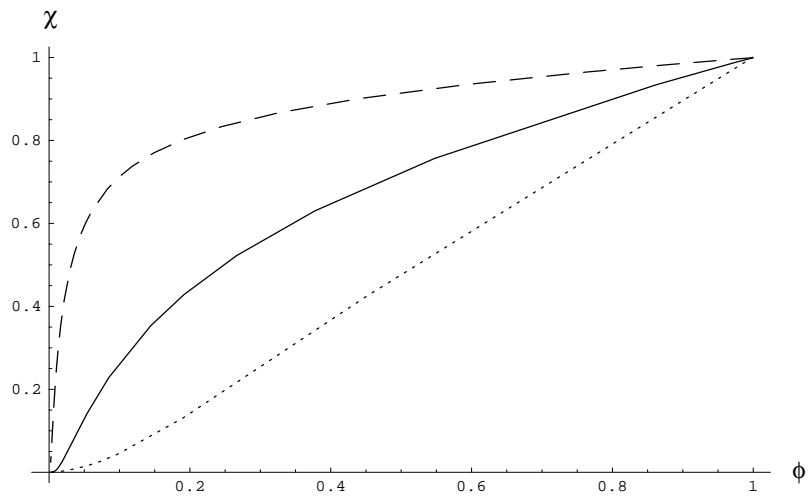


Figure 1: Real walls ($N = 3$). The parametric plots for $m = 1$ (solid line), $m = .1$ (dashed line), and $m = 10$ (dotted line). ϕ and χ are measured in units of R_* and ρ_* , respectively.

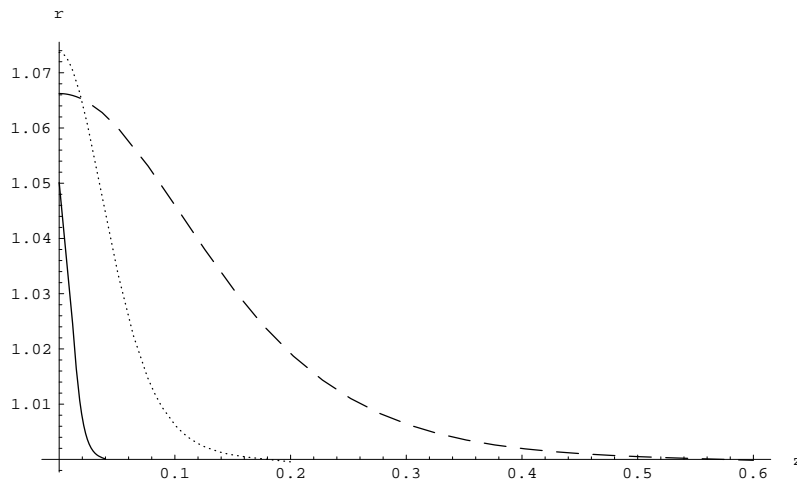


Figure 2: BPS walls in Higgs phase for $N = 3$ (dashed line), $N = 5$ (dotted line) and $N = 10$ (solid line).

(z_0 is the position of the wall center). For $N \geq 3$, the solutions can be found numerically. The profiles for the ratio $r(z) = \rho(z)/\rho_*$ in the interval $z_0 \equiv 0 \leq z < \infty$ [it is a half of the wall, another half being restored by symmetry considerations: $\rho(-z) = \rho(z)$] with different $N = 3, 5, 10$ are presented in Fig. 2.

We see that the dependence $\rho(z)$ is not flat anymore but displays a bump in the middle. To understand it, remind that the system (4.3) has the integral of motion (2.11). In our case, it amounts to

$$\frac{m(N-1)}{2} \rho^2 \cos \gamma - \frac{2}{3\rho^{2(N-1)}} \cos[\gamma(N-1)] = \frac{N}{2} \left(\frac{4m^{N-1}}{3} \right)^{1/N} \cos \frac{\pi}{N} \quad (4.6)$$

as follows from the boundary conditions (4.2) and the relations (2.8). In the middle of the wall, $\gamma = 0$, and the condition (4.6) implies

$$(N-1)x^2 - \frac{1}{x^{2(N-1)}} = N \cos \frac{\pi}{N} \quad (4.7)$$

($x \equiv r(0)$). It is not difficult to observe that the real root of the algebraic equation (4.7) is slightly greater than 1 for $N \geq 3$. When N is large, $x - 1$ tends to zero $\propto 1/N$.

5 Born – Oppenheimer Expansion at Small Masses

When $m \neq 0$, the gauge degrees of freedom associated with the superfield Φ do not decouple completely and should be taken into account. The full system (3.1) of the BPS equations for the complex domain walls has the form

$$\begin{aligned} \rho' &= (N-1) \left[m\rho \sin(2\alpha - \pi/N) - \frac{4R^3}{3\rho} \sin(3\beta - \pi/N) \right] \\ \alpha' &= (N-1) \left[m \cos(2\alpha - \pi/N) - \frac{4R^3}{3\rho^2} \cos(3\beta - \pi/N) \right] \\ R' &= -2R^2 \left[\sin(3\beta - \pi/N) \ln(R^3 \rho^{2(N-1)}) + \cos(3\beta - \pi/N) [3\beta + 2\alpha(N-1)] \right] \\ \beta' &= 2R \left[-\cos(3\beta - \pi/N) \ln(R^3 \rho^{2(N-1)}) + \sin(3\beta - \pi/N) [3\beta + 2\alpha(N-1)] \right] \end{aligned} \quad (5.1)$$

where, as in the previous section, we have chosen $\delta = \pi/N - \pi/2$ and introduced the polar variables $\chi = \rho e^{i\alpha}$, $\phi = R e^{i\beta}$. One should solve the system (5.1) with the boundary conditions

$$\begin{aligned} \rho(-\infty) &= \rho(\infty) = \rho_*; & R(-\infty) &= R(\infty) = R_*; \\ \alpha(-\infty) &= \beta(-\infty) = 0; & \alpha(\infty) &= \pi/N; & \beta(\infty) &= -\frac{2(N-1)\pi}{3N} \end{aligned} \quad (5.2)$$

When $N = 2$, the system (5.1) is reduced to that studied in Refs.[10, 11].

Generally, we should solve the full system (5.1) numerically. The problem is simplified when noting that the wall solution should be symmetric with respect to

its center. Let us seek for the solution centered at $z = 0$ so that

$$\begin{aligned} \rho(z) &= \rho(-z), \quad R(z) = R(-z), \\ \alpha(z) &= \pi/N - \alpha(-z), \quad \beta(z) = -2(N-1)\pi/(3N) - \beta(-z) \end{aligned} \quad (5.3)$$

Indeed, one can be easily convinced that the Ansatz (5.3) goes through the equations (5.1). It is convenient to solve the equations (5.1) numerically on the half-interval from $z = 0$ to $z = \infty$. The symmetry (5.3) dictates $\alpha(0) = \pi/(2N)$, $\beta(0) = -(N-1)\pi/(3N)$. The values $\rho(0)$ and $R(0)$ are related by the condition (2.11) which reads here

$$\frac{4R^3(0)}{3} \left\{ \ln[R^3(0)\rho^{2(N-1)}(0)] - 1 \right\} + m\rho^2(0)(N-1) = N \left(\frac{4m^{N-1}}{3} \right)^{1/N} \cos \frac{\pi}{N} \quad (5.4)$$

Thus, only one parameter at $z = 0$ [say, $R(0)$] is left free. We should fit it so that the solution would approach the values specified in Eq.(5.2) at $z \rightarrow \infty$. The numerical solution for this problem will be presented and discussed in the next section. Here we will concentrate on the case when m is small where some analytic results can be obtained.

In the limit $m \rightarrow 0$, we can just freeze the heavy variables:

$$\beta = -2\alpha(N-1)/3; \quad R = \rho^{-2(N-1)/3} \quad (5.5)$$

in which case the first two equations in Eq.(5.1) reproduce the system (4.3) studied in the previous section. This is the leading order of the Born–Oppenheimer expansion. To proceed further, we should allow for the fast variables R , β to deviate from their zero order values (5.5). Integrating these deviations out, one can obtain the corrections to the leading order Born–Oppenheimer hamiltonian for the slow variables ρ , α . The spectrum of the low–energy effective hamiltonian and all other quantities of interest can be expanded in a series over a small parameter. In our case, the relevant expansion parameter is $\sim m/R_* \propto m^{(2N+1)/3N}$.

Such an expansion can be carried out also on the level of dynamic equations. One should present

$$\rho = \rho_0 + \rho_1 + \rho_2 + \dots, \quad \alpha = \alpha_0 + \alpha_1 + \alpha_2 + \dots, \quad R = R_0 + R_1 + R_2 + \dots, \quad \beta = \beta_0 + \beta_1 + \beta_2 + \dots$$

, where ρ_0 and α_0 are the solutions of the system (4.3) and R_0 , β_0 are found from Eq.(5.5), and linearize the equations in each subsequent order. Let us do it for the BPS system (5.1). We will be particularly interested in the quantity $R(0)$ to compare it with the numerical results of the next section.

Let us look first at the two last equations in Eq.(5.1). In the first non-trivial order, we have

$$\begin{aligned} R'_0 &= -2R_0^2 \left\{ \sin(3\beta_0 - \pi/N) \left[\frac{3R_1}{R_0} + \frac{2(N-1)\rho_1}{\rho_0} \right] + \cos(3\beta_0 - \pi/N) [3\beta_1 + 2\alpha_1(N-1)] \right\} \\ \beta'_0 &= 2R_0 \left\{ -\cos(3\beta_0 - \pi/N) \left[\frac{3R_1}{R_0} + \frac{2(N-1)\rho_1}{\rho_0} \right] + \sin(3\beta_0 - \pi/N) [3\beta_1 + 2\alpha_1(N-1)] \right\} \end{aligned} \quad (5.6)$$

From this, one can readily express R_1 and β_1 to be substituted in the linearized version of the first pair of the equations in Eq.(5.1). As a result, we obtain the linear system for ρ_1 and $\gamma_1 = 2\alpha_1 - \pi/N$:

$$\begin{aligned}
\rho_1' &= (N-1) \left\{ -\frac{4(N-1)}{9} \rho_0^{-2(2N+1)/3} \rho_1' + \rho_1 \left[m \sin \gamma_0 + \frac{4(2N-1)}{3\rho_0^{2N}} \sin[\gamma_0(N-1)] \right] + \right. \\
&\quad \left. \gamma_1 \left[m\rho_0 \cos \gamma_0 - \frac{4(N-1)}{3\rho_0^{(2N-1)}} \cos[\gamma_0(N-1)] \right] \right\} \\
\gamma_1' &= 2(N-1) \left\{ -\frac{2(N-1)}{9} \rho_0^{-2(2N+1)/3} \gamma_1' - \frac{8N}{3\rho_0^{(2N+1)}} \cos[\gamma_0(N-1)] \rho_1 - \right. \\
&\quad \left. -\gamma_1 \left[m \sin \gamma_0 + \frac{4(N-1)}{3\rho_0^{2N}} \sin[\gamma_0(N-1)] \right] \right\},
\end{aligned} \tag{5.7}$$

The proper initial conditions for this system at the middle of the wall are

$$\rho_1(0) = 0, \quad \gamma_1(0) = 0 \tag{5.8}$$

The fact that the value of the phase in the middle is not shifted is a trivial corollary of the symmetry conditions (5.3). To understand why also $\rho(0)$ is not shifted, one should look at the relation (5.4). Linearizing it with respect to $R(0)$, $\rho(0)$, we observe that the partial derivative of the left-hand side over $R(0)$ is zero for the 0th order solution while the derivative over $\rho(0)$ is not. Hence, $\rho_1(0) = 0$, indeed. When the initial conditions (5.8) are posed, the solutions $\rho_1(z)$, $\alpha_1(z)$ of the system (5.7) should approach zero at $z \rightarrow \infty$. We checked numerically that they do.

Bearing in mind that $\rho_1(0) = 0$, it is easy to find what $R_1(0)$ is. For $z = 0$, the second equation in (5.6) is reduced to

$$R_1(0) = \frac{\beta_0'(0)}{6} = -\frac{(N-1)^2}{9} \left[m + \frac{4}{3\rho_0^{2N}(0)} \right] \tag{5.9}$$

where the relation (5.5) and the second equation in Eq.(4.3) were used. To find the shift in the next order, one should expand the equation for $\beta'(0)$ further. We obtain

$$\beta_1'(0) = 6R_2(0) + \frac{3R_1^2(0)}{R_0(0)} + \frac{4(N-1)R_0(0)}{\rho_0(0)} \rho_2(0) \tag{5.10}$$

The second order shift in $\rho(0)$ can be found from the expansion of Eq.(5.4):

$$\rho_2(0) = -\frac{3R_0(0)R_1^2(0)}{(N-1)\rho_0(0)[m + \frac{4R_0^3(0)}{3\rho_0^2(0)}]} \tag{5.11}$$

$\beta_1'(0)$ can be found by differentiating the solution of the linear algebraic system (5.6) at $z = 0$. Using Eqs.(4.3, 5.5) again and combining everything, we arrive at the final

result

$$\begin{aligned} \eta(m) = \frac{R(0)}{R_0(0)} = 1 - \frac{(N-1)^2}{9R_0(0)} \left[m + \frac{4}{3\rho_0^{2N}(0)} \right] - \\ \frac{(N-1)^3}{162R_0^2(0)} \left[m + \frac{4}{3\rho_0^{2N}(0)} \right] \left[m(7N-1) - \frac{32(N-1)}{3\rho_0^{2N}(0)} \right] + \\ O[m^3/R_0^3(0)] \end{aligned} \quad (5.12)$$

For $N = 2$ when $\rho_0(0) = \rho_*$ and $R_0(0) = R_*$, the expression simplifies [11]:

$$\eta(m) = 1 - \frac{2}{9} \left(\frac{4m^5}{3} \right)^{1/6} - \frac{5}{81} \left(\frac{4m^5}{3} \right)^{1/3} + O(m^{5/2}) \quad (5.13)$$

6 Two BPS solutions and Phase Transition in Mass

When m is neither too large nor too small, the Born–Oppenheimer approximation does not apply and we are in a position to solve the full system of 4 equations (5.1) numerically. We did it for $N = 3$ and $N = 4$. As was mentioned in the previous section, we use the symmetry relations (5.3) which fix the initial conditions at the middle of the wall for the phases and the relation (5.4) between $\rho(0)$ and $R(0)$ so that only one free parameter is left. We fit it so that the solution would tend to the vacuum values (5.2) when $z \rightarrow \infty$.

The situation turned out to be pretty much analogous to what happens at $N = 2$. First of all, the solutions exist only in a limited range of masses. When m is larger than some critical value m_* , the integral trajectory always *misses* the vacuum (5.2) no matter what value for $R(0)$ is chosen. Second, when $m < m_*$, there are not one, but *two* different solutions with a larger and a smaller value of $R(0)$. In Figs. 3, 4 we plotted the dependence of $\eta = R(0)/R(\infty)$ on m for both branches. We see that, at $m = m_*$, two branches are joined together. This *is* the reason why no solution exists at larger masses.⁴

The value of the critical mass m_* for higher unitary groups turned out to be much smaller than that for the $SU(2)$ theory:

$$m_*^{SU(3)} = .28604\dots; \quad m_*^{SU(4)} = .07539\dots \quad (6.1)$$

as compared to $m_* = 4.67059\dots$ for $SU(2)$.

Let us discuss now what happens with these two branches in the small mass limit. Consider first the upper branch. The illustrative profiles $\rho(z)/\rho_*$ in the $SU(3)$ theory for the upper branch at $m = .1$ and for $m = m_* = .28604$ (when the solution is unique) are plotted in Fig. 5. Comparing the dashed curves in Fig. 5 and Fig. 2, we see that, for small masses, the solution approaches, as it should, the “Higgs wall”

⁴The presence of two solutions at $m < m_*$ and their absence at $m > m_*$ can be naturally understood by making some simple observations on the phase portrait of the system (5.1) [11].

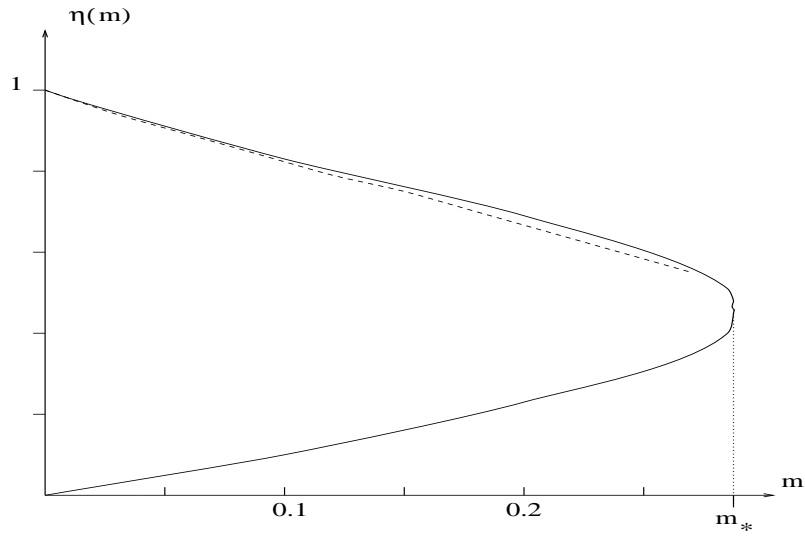


Figure 3: The ratio $\eta = R(0)/R_0(0)$ as a function of mass for the $SU(3)$ theory. The dashed line describes the analytic result (5.12) valid for small masses.

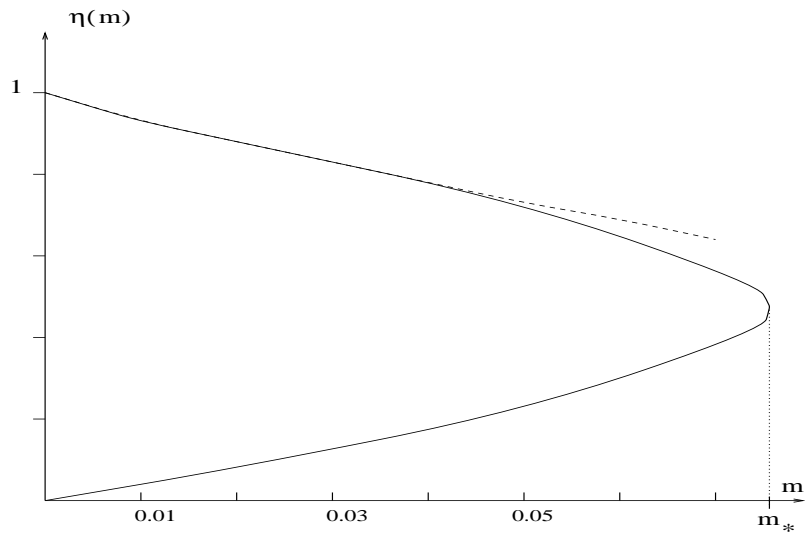


Figure 4: The same as Fig. 3 for the $SU(4)$ theory.

solution studied in Sect. 4. The numerical findings for $\eta(m)$ are in an excellent agreement with the approximal analytic result (5.12) both for $SU(3)$ and for $SU(4)$.

The result (5.12) allows one to understand why the values of m_* fall down with N and to make an estimate of m_* at large N . Indeed, the critical mass m_* and the value of the mass where the Born–Oppenheimer expansion in Eq.(5.12) breaks down should be of the same order. For large N , the expansion parameter is $\kappa \sim N^2(m/R_*) \sim N^2m^{2/3}$. Assuming $\kappa \sim 1$, we arrive at the conclusion that m_* falls down as

$$m_*(N) \propto N^{-3}$$

in the limit $N \rightarrow \infty$.

The lower BPS branch is something new which was not and could not be seen in the framework of the effective Higgs theory (2.17). The latter was obtained by freezing down to zero the logarithm in the full potential (2.5). But, as was already mentioned, we could equally well set $\phi = 0$. Actually, we see, indeed, that $R(0) \rightarrow 0$ when $m \rightarrow 0$ for the lower branch, i.e. the solution passes in the vicinity of the chirally symmetric vacuum on its way from one chirally asymmetric vacuum to another.

A similar lower BPS solution exist also for $N = 2$, but in that case it is much simpler approaching in the limit $m \rightarrow 0$ a combination of two *real* walls separated at a large distance (The phases $\alpha(z)$ and $\beta(z)$ are changed, of course, so that the whole solution is complex, but the change occurs in the central region where the absolute values of the fields R and ρ are very small.). For $N \geq 3$, it cannot be true because the energy of a complex BPS wall is not just twice the energy of a complex BPS wall, but is lower. One can say that, at small masses, two real BPS walls with the energy (2.12) attract each other at large distances and two different bound states with the same energy (2.13) are formed. ⁵

7 Lower BPS branch at small masses

The properties of this new complex BPS branch are rather peculiar. They are worth studying in some details. As was also the case for the real walls, this solution penetrates a high and narrow potential barrier so that the central region of the wall finds itself in the vicinity of the chirally symmetric vacuum. However, in contrast to the case $N = 2$, it always passes the minimum $\phi = \chi = 0$ at a finite distance: though $\lim_{m \rightarrow 0} R(0)$ is zero, $\lim_{m \rightarrow 0} \rho(0)$ is not. This can be immediately seen from

⁵This terminology looks somewhat artificial in 4 dimensions where the walls have infinite energy involving the area factor, but one could equally well discuss a 2-dimensional $\mathcal{N} = 2$ supersymmetric Wess–Zumino model with the superpotential (2.4) in which case the walls are interpreted as solitons and the wall spectrum is just *the* spectrum, at least an essential part of it (there may be also some breathers). E.g., for $N = 3$ and $m < m_*$, we have in our disposal 6 real bosonic solitons and antisolitons with the mass ϵ_r and twice as much complex bosonic solitons and antisolitons with the mass $\sqrt{3}\epsilon_r$, each soliton possessing a superpartner associated with the fermion zero mode dwelling on the wall. One may wonder whether the model is exactly solvable in Zamolodchikov’s sense ?

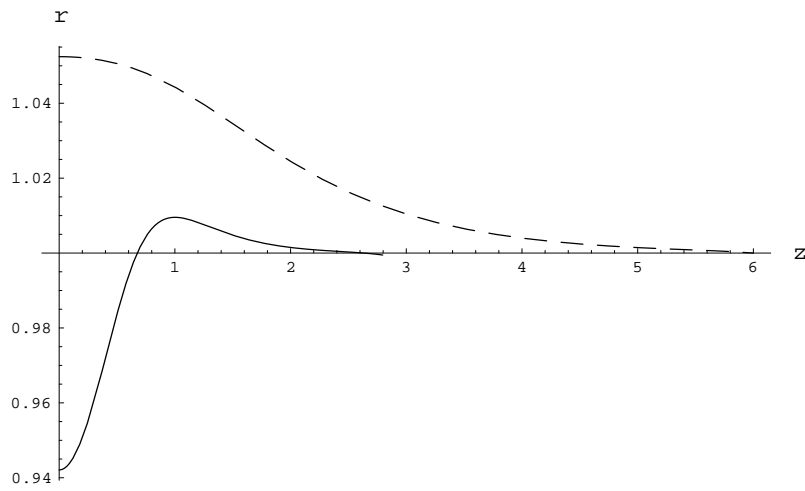


Figure 5: The ratio $r(z) = \rho(z)/\rho_*$ in the $SU(3)$ theory as a function of z for $m = m_*$ (solid line) and for the upper BPS branch at $m = .1$ (dashed line).

the relation (5.4). For $N \geq 3$, the right-hand side is non-zero, and, when $R(0) \rightarrow 0$, $\rho(0)$ tends to the value

$$\rho_{m=0}(0) \equiv \rho_0 = \sqrt{\frac{N \cos \frac{\pi}{N}}{N-1}} \left(\frac{4}{3m}\right)^{1/2N} = \sqrt{\frac{N \cos \frac{\pi}{N}}{N-1}} \rho_* \quad (7.1)$$

Let us look first at the numerical solution for $\rho(z)$ and $R(z)$ for the lower BPS wall at $N = 3$, $m = .01$ shown in Figs. 6, 7. We see that the wall consists of three distinct regions. First, when going out from the middle point, $\rho(z)$ goes gradually up while $R(z)$ stays practically at zero. Then, in the intermediate region, $R(z)$ changes rather abruptly while $\rho(z)$ is practically not changed. Finally, $\rho(z)$ and $R(z)$ change together in a smooth concerted way until the trajectory levels off at the asymmetric vacuum values ρ_* and R_* .

This complicated pattern can be understood and described analytically. The analysis is quite parallel to what has been done earlier for the real walls. In the limit $m \rightarrow 0$ and while $R(z)$ stays small as is the case in the central wall region, the system (5.1) is greatly simplified and acquires the form

$$\begin{cases} \rho' = (N-1)m\rho \sin \gamma \\ \gamma' = 2(N-1)m \cos \gamma \end{cases} \quad (7.2)$$

It has the analytic solution

$$\begin{cases} \rho(z) = \rho_0 \cosh^{1/2}[2m(N-1)z] \\ \sin \gamma(z) = \tanh[2m(N-1)z] \end{cases} \quad (7.3)$$

Indeed, the numerical solutions for $\rho(z)$ and $\gamma(z)$ follow the formulae (7.3) rather closely up to the turning point at $z \approx 20$. On the other hand, for the outer region of the wall we are in the Higgs region. The fields $R(z)$ and $\beta(z)$ are frozen as is dictated by Eq.(5.5), and it is the equation system (4.3) rather than Eq.(7.2) which describes the wall dynamics. The change of the regime occurs when the trajectory (7.3) intercepts the integral trajectory of Eq.(4.3). For $N \geq 3$, the dependencies $\rho(z)$ and $\gamma(z)$ in the Higgs phase can be found only numerically, but the trajectory in the (ρ, γ) plane is described analytically according to Eq.(4.6). The interception occurs at

$$\rho_\times = \frac{\rho_0}{\sqrt{\cos \frac{\pi}{2(N-1)}}}, \quad \gamma_\times = \frac{\pi}{2(N-1)} \quad (7.4)$$

In the transitional region, we should fix instead $\rho(z)$ and $\alpha(z) = \gamma(z)/2 + \pi/(2N)$ to their values in Eq.(7.4) after which the system (5.1) is reduced to

$$R' = -2R^2 \ln[R^3 \rho_\times^{2(N-1)}] \quad (7.5)$$

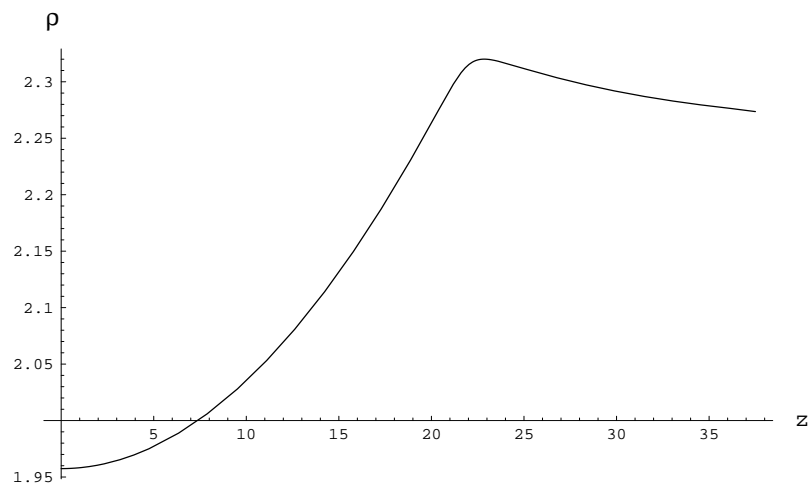


Figure 6: Profile $\rho(z)$ of the lower BPS branch at $N = 3$, $m = 0.01$

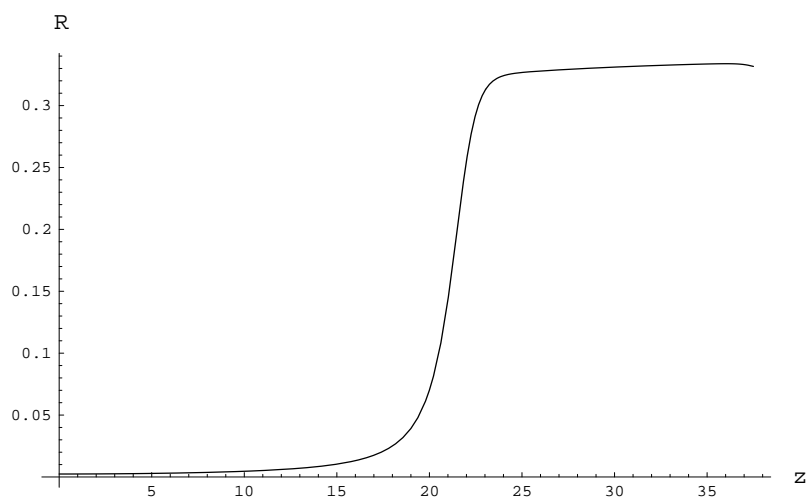


Figure 7: Profile $R(z)$ of the lower BPS branch at $N = 3$, $m = 0.01$.

and β is fixed at the value

$$\beta_{\times} = -\frac{N-1}{3} \left(\gamma_{\times} + \frac{\pi}{N} \right) = \frac{\pi}{3N} - \frac{\pi}{2} \quad (7.6)$$

After a trivial rescaling, the equation (7.5) just coincides with the BPS equation (3.2) describing the real wall in pure supersymmetric gluodynamics. As was the case for the real walls, the transitional region, the region where the potential barrier between the Higgs phase $\phi = \chi^{-2(N-1)/3}$ and the symmetric phase $\phi = 0$ is penetrated, is rather narrow. Its width in z is of order $\rho_{\times}^{2(N-1)/3} \propto m^{-(N-1)/3N}$. On the other hand, the characteristic width of the central and of the outer region is large $\propto 1/m$.

Note that, for $N = 2$ when our wall is a superposition of two distant real walls, its structure is simpler. A wide outer region is absent simply because the values (7.4) where the transition occurs coincide in this case with the asymmetric vacuum values. But the wide central region and the narrow transitional region are still there.

The full energy of the configuration described coincides, of course, for small masses with the BPS bound (2.13). One can find out that the fractions of the wall energy f_c , f_{trans} , and f_{out} carried, correspondingly, by the central region, the transitional region, and the outer region are ⁶

$$\begin{aligned} f_c &= \frac{\tan \frac{\pi}{2(N-1)}}{\tan \frac{\pi}{N}}, & f_{\text{trans}} &= \frac{1}{N \sin \frac{\pi}{N}} \left[\frac{(N-1) \cos \frac{\pi}{2(N-1)}}{N \cos \frac{\pi}{N}} \right]^{N-1}, \\ f_{\text{out}} &= 1 - f_c - f_{\text{trans}}. \end{aligned} \quad (7.7)$$

For $N = 3$, $f_c \approx .58$, $f_{\text{trans}} \approx .34$, and $f_{\text{out}} \approx .08$.

8 Discussion

Our main result is that, while the real BPS domain walls connecting the chirally symmetric and a chirally asymmetric vacua are present at all masses, the complex BPS walls interpolating between different asymmetric vacua exist only for small enough masses $m < m_*$, m_* being given in Eq.(6.1). A kind of phase transition associated with the restructuring of the wall spectrum occurs. ⁷ It makes sense to express the result in invariant terms and to trade Λ_{SQCD} for an invariant physical quantity such as the gluino condensate $\Sigma = | \langle \text{Tr } \lambda^2 \rangle |$ in a chirally asymmetric vacuum. Restoring the dimensional factor $\Lambda_{SQCD}^{(2N+1)/N}$ in Eqs.(1.2, 2.9) and combining it with Eq.(6.1), we obtain

$$m_*^{SU(3)} \approx .085 \Sigma^{1/3}, \quad m_*^{SU(4)} \approx 0.033 \Sigma^{1/3} \quad (8.1)$$

⁶To avoid confusion, note that, by derivation, this result is valid only for $N \geq 3$.

⁷Needless to say, it is not a phase transition of a habitual thermodynamic variety. In particular, the vacuum energy is zero both below and above the phase transition point — supersymmetry is never broken here. Hence $E_{\text{vac}}(m) \equiv 0$ is not singular at $m = m_*$.

We cannot, however, claim that the *quantitative* estimates in Eq.(8.1) are, indeed, quite correct. The matter is that the particular values of the factors in Eq.(8.1) are sensitive to the form of the kinetic term in the effective lagrangian which, in contrast to the potential term, is not fixed rigidly by symmetry considerations. Just multiplying, say, the standard kinetic term for the X superfield $\mathcal{L}_{\text{kin}}^X = 1/4 \int d^4\theta \bar{X}X$ by a numerical factor would change the particular values (8.1) of m_* [11]. The effective lagrangian may also involve complicated kinetic structures with higher field derivatives $\propto (\partial\phi)^4$ etc.

The effective TVY lagrangian *implies* the presense of the chirally invariant phase [3]. Recently, this conclusion has been criticized [15, 16]. In particular, it was shown in Ref.[15] that the *assumption* that the spectrum of the chirally symmetric phase in the supersymmetric gluodynamics involves the massless particles associated with the colorless composite field Φ in the effective lagrangian does not conform with the 't Hooft anomaly matching conditions of some global discrete anomalies.

However, this does not exclude the possibility that the chirally symmetric phase still exists, but its spectrum has nothing to do with that extracted from the naive VY effective lagrangian with the standard kinetic term. Indeed, for the dimension of the above mentioned terms with higher derivatives of ϕ to be correct, they should involve some powers of ϕ in the denominator (no new dimensionful constants can be introduced: that would spoil the conformal properties of the lagrangian). The presense of such singular terms would modify the spectrum of the chirally symmetric phase completely [17]. Actually, the dynamics of the symmetric phase is quite unclear by now. This is an extremely interesting problem to solve but, at the moment, we do not have insights in this direction.

We want to emphasize, however, that though higher-derivative singular terms may destroy completely a naive spectrum picture, they do not affect the conclusion on the *existence* of the symmetric phase. When the fields are *static and homogeneous*, the form of the effective lagrangian is extracted quite rigidly from the requirement that the conformal and chiral anomaly of the original theory are reproduced correctly. Also, the dynamics of the domain walls depend largely on the region *between* the vacua where the extra terms with higher derivatives are not singular. Thereby, they should not modify the structure of the walls revealed in Refs.[5, 10, 11] and in this paper. At least, this is our guess and hope. In particular, a *qualitative* conclusion on the absence of a smooth transition between the small mass region and the large mass region in supersymmetric QCD *is* correct.

In this paper, we studied only the BPS solutions, but, as it was done earlier for $SU(2)$ [11], one may and actually should study also non-BPS walls, the field configurations which satisfy the equations of motion but not the first-order BPS equations. This work is now in progress [18]. Our preliminary results display that the picture is roughly the same as for $SU(2)$: in some range of masses $m_* < m \leq m_{**}$, a non-BPS complex domain wall presenting a local minimum of the energy functional exists. There are also sphaleron wall solutions. For $m > m_{**}$, the complex walls disappear altogether from the spectrum.

Acknowledgments: I acknowledge illuminating discussions with A. Kovner and A.I. Veselov and warm hospitality extended to me at Saclay where this work was finished. This work was supported in part by the RFBR–INTAS grants 93–0283 and 94–2851, by the RFFI grant 97–02–16131, by the U.S. Civilian Research and Development Foundation under award # RP2–132, and by the Schweizerischer National Fonds grant # 7SUPJ048716.

References

- [1] N. Seiberg and E. Witten, *Nucl. Phys.* **B426** (1994) 19; (E) **B430** (1994) 485.
- [2] V. Novikov, M. Shifman, A. Vainshtein, and V. Zakharov, *Nucl. Phys.* **B229** (1983) 407; *Phys. Lett.* **B166** (1986) 334; I. Affleck, M. Dine and N. Seiberg, *Nucl. Phys.* **B241** (1984) 493; **B256** (1985) 557. G. Rossi and G. Veneziano, *Phys. Lett.* **138B** (1984) 195; D. Amati, K. Konishi, Y. Meurice, G. Rossi and G. Veneziano, *Phys. Rep.* **162** (1988) 169; M. Shifman, *Int. J. Mod. Phys.* **A11** (1996) 5761.
- [3] A. Kovner and M. Shifman, hep-th/9702174 [Phys. Rev. D, to appear].
- [4] G. Dvali and M. Shifman, *Phys. Lett.* **B396** (1997) 64; hep-th/9611213 [Nucl. Phys. B, to appear].
- [5] A. Kovner, M. Shifman, and A. Smilga, hep-th/9706089 [Phys. Rev. D, to appear].
- [6] E. Witten and D. Olive, *Phys. Lett.* **B78**(1978) 97.
- [7] S. Cecotti and C. Vafa, *Commun. Math. Phys.* **158** (1993) 569.
- [8] E. Abraham and P. Townsend, *Nucl. Phys.* **B351** (1991) 313; M. Cvetič, F. Quevedo, and S.-J. Rey, *Phys. Rev. Lett.* **67** (1991) 1836.
- [9] B. Chibisov and M. Shifman, hep-th/9706141.
- [10] A. Smilga and A. Veselov, hep-th/9706217 [Phys. Rev. Lett., to appear].
- [11] A. Smilga and A. Veselov, hep-th/9710123.
- [12] T. Taylor, G. Veneziano and S. Yankielowicz, *Nucl. Phys.* **B218** (1983) 493.
- [13] G. Veneziano and S. Yankielowicz, *Phys. Lett.* **113B** (1982) 231.
- [14] A. Smilga, *Phys. Rev.* **D54** (1996) 7757.
- [15] C. Csaki and H. Murayama, hep-th/9710105.

- [16] M. Schwetz and M. Zabzine, hep-th/9710125.
- [17] This remark belongs to A. Kovner.
- [18] A.V. Smilga and A.I. Veselov, in preparation.